

# Co-ordination and intermediate-range order alterations in densified germania

M. Micoulaut<sup>a</sup>, X. Yuan<sup>b</sup>, L.W. Hobbs<sup>b,\*</sup>

<sup>a</sup> *Laboratoire de Physique Théorique de la Matière Condensée, Université Pierre et Marie Curie, CNRS UMR 7600, Boite 121, 4 Place Jussieu, 75252 Paris cedex 05, France*

<sup>b</sup> *Massachusetts Institute of Technology, 77 Massachusetts Avenue, Cambridge, MA 02139-4307, USA*

Available online 2 April 2007

## Abstract

We analyze the structure of a-GeO<sub>2</sub>, pressure-densified from a starting density of 3660 kg/m<sup>3</sup> to a final density of 6000 kg/m<sup>3</sup>, using a combination of molecular dynamics simulation and topological analysis employing efficient local cluster ring counting algorithms. The initial modeled configuration is dominated by fourfold germanium co-ordination and rings of six or seven germanium atoms (as in cristobalite- or tridymite-like a-SiO<sub>2</sub>). The first response to increasing density is a change to larger ring (e.g. 8-ring) configurations (as in quartz-like a-SiO<sub>2</sub>) that pack more compactly. At still higher pressure, an intermediate fivefold germanium co-ordination appears that progressively converts into almost entirely sixfold (octahedral) germanium at higher pressures, accompanied by growth of the 3- and 4-rings that characterize the rutile-GeO<sub>2</sub> crystalline polymorph. The topology of the final densified structure does not entirely resemble a rutile-like glass analogue, however, because of the retention of 6-rings and almost 10% 5-co-ordinated Ge. Overall, the present study shows how pressure (or density) affects the structure of the glass at a range of length scales.

© 2007 Elsevier B.V. All rights reserved.

PACS: 61.43.Bn; 61.43.Fs; 61.50.Ks; 81.05.Kf

Keywords: Pressure effects; Molecular dynamics; Germania; Long-range order; Medium-range order; Short-range order

## 1. Introduction

Properties of network glasses appear to depend strongly on the intermediate-range order of their backbones. In the past five years, sophisticated advances in traditional diffraction methods (X-ray, neutron scattering) have been employed in attempts to quantify both the local structure (successfully) and intermediate-range structure (largely unsuccessfully) in densified glasses that have been subjected to applied pressure [1–4]. While molecular simulation models can be evaluated easily for their local structure, efficient topological algorithms are needed to quantify the intermediate-range order generated, most simply through application of network ring analysis and local cluster identification

[5]. Rings are a necessary steric consequence of avoiding tree-like networks that would increase exponentially in density as they grow; even though such circuits do not tessellate three-dimensional structures, their topology is remarkably sensitive to structural changes at intermediate-range. This paper shows that the topology evolves with pressure (or density) and that the way the distribution of rings evolves depends very much on their size and the co-ordination changes. These new ideas on the relationship between pressure and topology in a network structure provide a framework for new interpretation of scattering data that go beyond simple short-range correlations.

Typical network oxide glasses, such as silica (SiO<sub>2</sub>) or germania (GeO<sub>2</sub>), exhibit striking alterations with applied pressure [6–8]. The local structure of these kinds of systems, which represent some of the best inorganic glass formers in nature, consists of almost-regular [MO<sub>4</sub>] (M = Si or Ge) short-range ordered tetrahedra joined through

\* Corresponding author. Tel.: +1 617 253 6835; fax: +1 617 252 1020.  
E-mail address: [hobbs@mit.edu](mailto:hobbs@mit.edu) (L.W. Hobbs).

sharing their oxygen vertices. Experimental data show that application of pressure has two effects: (1) the density increases but exhibits hysteresis on removal of pressure [9]; and (2) ultimately a change in short-range co-ordination occurs, from the  $[\text{MO}_4]$  tetrahedral local structure to the  $[\text{MO}_6]$  octahedral local co-ordination that is a feature of high pressure (rutile-like) crystalline phases [10]. The tetrahedral-to-octahedral co-ordination conversion can be traced rather easily by following the interatomic bond lengths, which show a marked jump at about 5 GPa (50 kbar) for  $\text{GeO}_2$  [11] or 13 GPa for  $\text{SiO}_2$  [12]. The resulting changes in bond lengths that exist throughout the network of the glass imply also that the intermediate-range order of the structural backbone has to be affected by the local order, as signaled by a shift and broadening of the first sharp diffraction peak (FSDP) with increasing pressure [12]. Recent experiments have now focused on germania because of its increased sensitivity to pressure change [13]. More details of  $\text{GeO}_2$  can be found in a recent review [14].

## 2. Simulation details and algorithms

Molecular dynamics simulations of a dense  $\text{GeO}_2$  glass were performed in the (N, V, E) ensemble, using a model in which 768 atoms interacted via an Elliott–Offner potential [15]. The latter potential appears to be reliable under progressive densification and has been used to study the local structure of permanently densified  $\text{GeO}_2$ . Details of the simulation can be found elsewhere [16,17]. In the present simulation, sets of co-ordinates were produced, ranging from the ordinary density of the glass at  $\rho = 3660 \text{ kg/m}^3$  ( $3.66 \text{ g/cm}^3$ ) [18] up to  $6000 \text{ kg/m}^3$  ( $6.00 \text{ g/cm}^3$ ). The latter corresponds to a glass under 22.82 GPa pressure (228 kbar), Table 1. Topological analysis of the resulting atomic co-ordinates was carried using the Yuan–Cormack (YC) ring counting algorithm [19], expanded from the original breadth-first search algorithm developed by Jesurum, Berger and Hobbs [5,20] and incorporated into the Net-Anal code package [21]. In contrast to other ring statistics algorithms developed for amorphous systems, the YC algorithm is designed to be particularly efficient at enumerating larger rings, identifying primitive rings and establishing the primitive ring content of every local cluster in an ensemble. For the purposes of ring counting, a network connection (i.e. chemical bond) was defined when the distance between a Ge and an O atom was less than the radius of the first minimum after the first co-ordination-shell peak in the pair-wise total correlation function.

Primitive rings, under the definition outlined by Mariani and Hobbs [22] are those network circuits that cannot be

decomposed into sets of two or more smaller rings, all of which are smaller than the original ring. A local primitive ring cluster (LPRC) is the set of all polytopes ( $[\text{GeO}_4]$  tetrahedra initially in this case) that are part of the set of primitive rings passing through any given polytope. Because the network polytopes will be seen to change progressively from  $[\text{GeO}_4]$  to  $[\text{GeO}_5]$  to  $[\text{GeO}_6]$  co-ordination polyhedra under pressure, it is more complete to count atom-based rings (the  $n$  steps along an  $n$ -ring ring circuit taken from atom-to-atom, without distinguishing atom type) and to define local clusters based on them. However, for simplicity (and because it is the more usual convention for tetrahedral glasses) we elect instead to define the ring steps as from one Ge atom to the next, where it is implicit that the circuit must go through intermediate oxygen atoms. The local primitive ring clusters defined are therefore Ge-centered, and a 2-ring in this notation is thus a shared edge between two Ge co-ordination polyhedra. Because the polyhedra change with Ge co-ordination, we elect to characterize the *size* of the local cluster by the number of *atoms*, rather than by number of polytopes, however. The atom and ring complements of local clusters associated with each Ge in the cristobalite-, quartz- and rutile-structure analogues of crystalline  $\text{GeO}_2$  are collated in Table 2. (Crystalline  $\text{GeO}_2$  appears to adopt only the quartz and rutile-structure types.) The Ge local cluster of the rutile-structure crystalline polymorph is illustrated in Fig. 1 and, as shown in Table 2, contains 2-rings (reflecting the edge-sharing octahedra of this structure) and dominant 4-rings.

## 3. Results

Fig. 2 shows the fraction of various germanium and oxygen co-ordination numbers as a function of model density. The data show that the conversion from tetrahedral to octahedral Ge co-ordination passes through an intermediate five-co-ordinated state that reaches a maximum at a density about  $5500 \text{ kg/m}^3$ , while tetrahedral co-ordination reaches minority status for densities larger than  $5000 \text{ kg/m}^3$ . At still higher density, octahedral  $[\text{GeO}_6]$  co-ordination becomes dominant. The corresponding oxygen co-ordination number (Fig. 2) shows that densification leads to an increase of three-co-ordinated species, while the fractions of one-co-ordinated (terminal non-bridging oxygen) and more exotic four-co-ordinated oxygen remain very low. Noteworthy is the fact that even at the normal density ( $3660 \text{ kg/m}^3$ ), there is a small number (less than 10%) of three-co-ordinated defect oxygens that grows with densification. We note also that these results parallel remarkably

Table 1  
Pressures sustained in the MD simulations at various densities

Density ( $\text{kg/m}^3$ )	3660	3800	4000	4500	5000	5500	6000
Pressure (GPa)	0.21	1.04	1.18	3.36	5.84	11.80	22.82

Table 2

Local Ge-centered local primitive ring cluster contents for ‘cristobalite-like’, quartz- and rutile-structure  $\text{GeO}_2$

‘Cristobalite- $\text{GeO}_2$ ’	Quartz- $\text{GeO}_2$	Rutile- $\text{GeO}_2$
69 atoms	155 atoms	53 atoms
Twelve 6-rings	Six 6-rings	Two 2-rings
	Forty 8-rings	Twelve 3-rings
		Twenty-four 4-rings

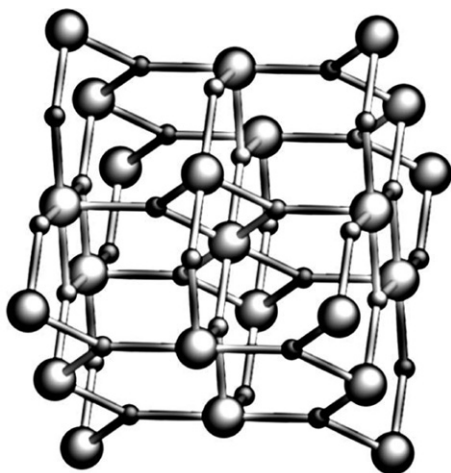


Fig. 1. Ge-centered (larger atoms) local cluster of  $\text{GeO}_2$  crystalline analogue of rutile. Analogous depictions of cristobalite-, tridymite- and quartz-structure local clusters can be found in Ref. [20].

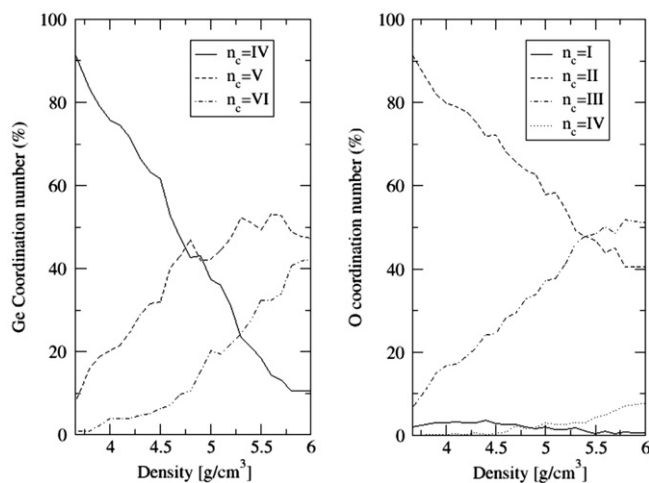


Fig. 2. Germanium and oxygen co-ordination numbers  $n_c$  as a function of density.

those obtained by Sharma and co-workers [23] from (N, P, T) ensemble molecular dynamics of  $\text{GeO}_2$ .

The ring analysis in Fig. 3 reveals that the densification of the structure leads to a global decrease of the average size of the local primitive ring clusters, dropping from almost 90 atoms in the starting glass at  $3660 \text{ kg/m}^3$  down to 66 atoms at  $5800 \text{ kg/m}^3$ , with a brief intermediate increase at around  $4500 \text{ kg/m}^3$  interrupting an otherwise

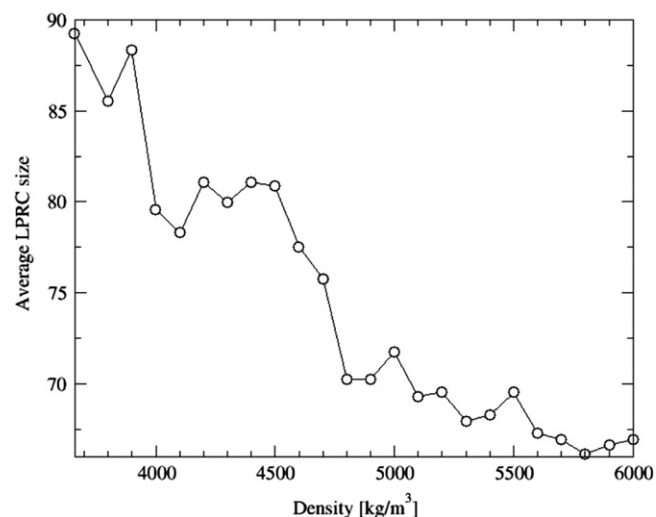


Fig. 3. Average Ge primitive ring cluster (LPRC) size found as a function of model density.

monotonic decline. Fig. 4 shows the ring distributions for the entire model at different densities; these differ slightly from the average ring distributions in local clusters. The size distribution peaks initially near 7-rings, then shifts with an increase in the population of 8- and 9-rings to an average closer to 8-rings, before shifting again to a peak at 6-rings at  $6000 \text{ kg/m}^3$ . Fig. 5 follows the ring populations of small rings (2- through 4-rings) and larger rings (5- through 7-rings) as a function of density in Ge-centered local clusters. Notable is the quadrupling of the number of 4-rings, the particularly sharp rise in 7-rings (and 8-rings) with increased pressure, and then their precipitous decrease and final supplanting by 6-rings above  $5500 \text{ kg/m}^3$ . The ring analysis provides unambiguous evidence for the strong effect of pressure effects on intermediate-range structure. As seen from both figures, smaller rings (including edge-sharing Ge co-ordination polyhedra signalled by 2-rings)

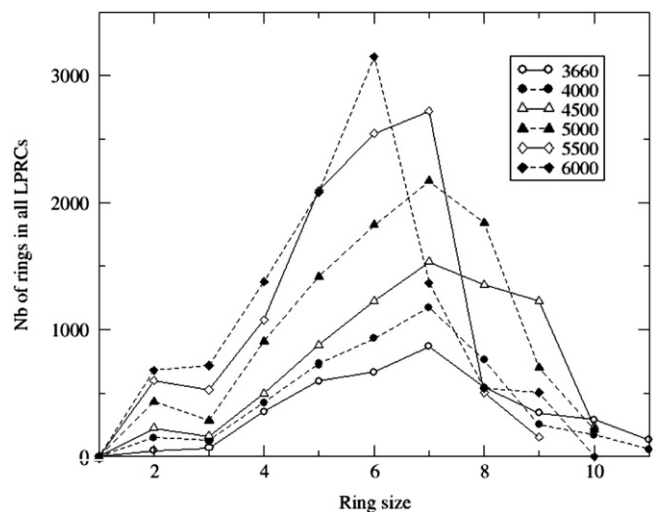


Fig. 4. Ring size distributions for densified  $\text{GeO}_2$  glasses at different model densities (in  $\text{kg/m}^3$ ).

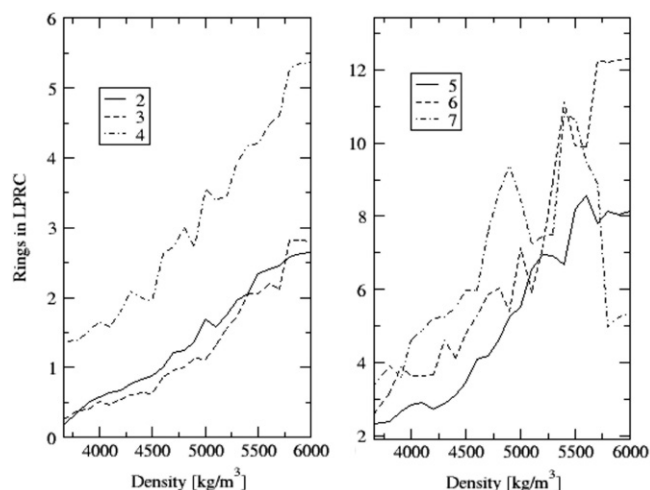


Fig. 5. Average ring counts for various size rings (2- through 7-rings) in local primitive clusters (LPRC) as a function of model density.

tend to increase, while the fraction of larger rings first increases then declines precipitously.

The ring distribution found by our method (Fig. 4) at ordinary density ( $3.66 \text{ kg/m}^3$ ) can be compared to the same distribution computed from a first-principles 168-atom model system of  $\text{GeO}_2$  using an alternative ring counting scheme [24]. Although our system is different, it is found that the profile of the small ring (3- and 4-rings) distributions is quite similar in the two models, whereas the higher ring fractions differ (the distribution in Ref. [24] peaks at  $n=6$ ). This result again implies that the larger rings reported are sensitive to the ring counting scheme. The rings counts for each model structure evaluated are, of course, exact. Topological evaluations of repeated MD simulation runs gave substantially the same results (within one standard deviation) as those displayed in Figs. 2–5.

#### 4. Discussion

These results are strongly suggestive that pressure does not act on intermediate-range structure in the same fashion as on short-range structure, and that identified classes of intermediate-range structure behave differently under application of pressure or density increase. Fig. 4 indicates that the average primitive ring size, which starts out near 7 at  $\rho = 3660 \text{ kg/m}^3$ , diminishes slightly with increasing density (the ring size for the cristobalite- or tridymite-structure phases of crystalline  $\text{GeO}_2$  is 6), but then with even more pressure (density) increases to 7.7 (the average ring size for the quartz-structure phase of crystalline  $\text{GeO}_2$ ). This behavior is consistent with previous topological analysis of silica [5,20,25], which shows that larger rings (like 8-rings) can accommodate higher density in these network structures because – unlike the smaller, more rigid and planar 6-rings – they can twist around and more efficiently fill space with atoms. The implication for  $\text{GeO}_2$  glasses is that, at low imposed density (low pressure), the intermediate-

range structure is initially dominated by 6- and 7-rings (intermediate between cristobalite- or tridymite-like and quartz-like, see Table 2), but that at higher imposed density (pressure) the intermediate-range network structure alters to one dominated more by larger 7-, 8-, and larger rings (quartz-like, or even resembling the highest pressure form of 4:2-connected crystalline silica, coesite [20]).

Above densities of  $5500 \text{ kg/m}^3$ , however, the average ring size decreases to 6. The average short-range co-ordination, shown in Fig. 2, increases – eventually to nearly 6:3 connectivity in which 6 O atoms surround each Ge atom and 3 Ge atoms surround each O atom, with the consequence that the resulting  $[\text{GeO}_6]$  octahedra must share some edges as well as vertices, as in the rutile-structure [26] of crystalline  $\text{TiO}_2$ . This is seen independently from the growth of the small 2-ring (edge-sharing Ge co-ordination polyhedra) in Fig. 4.

Experimentally, there have been some identifications of typical ring-breathing modes in Raman spectra of  $\text{GeO}_2$  [27], following the pioneering work of Galeener [28], that have been definitively attributed, on the basis of first-principles calculations [29], to localized vibrations of small rings in silica. Raman bands  $D_2$  and  $D_1$  at  $520 \text{ cm}^{-1}$  and  $420 \text{ cm}^{-1}$  are, indeed, thought to be respectively related to 3- and 4-rings. Wolf and co-workers have studied the evolution of the Raman spectra [30] with pressure, but conclusions about the 3- and 4-ring populations cannot be drawn, because the peak position changes with pressure. A recent analysis from first principles calculations [24,31] notably suggests that the  $D_2$  line at  $520 \text{ cm}^{-1}$  is indeed related to O breathing vibrations in three-membered rings. On the other hand, the same study suggests that the ‘4-membered ring’ line at  $420 \text{ cm}^{-1}$  seems to be rather a result of bond-bending modes, whereas the true four-membered rings contribute to the main Raman peak found around  $400 \text{ cm}^{-1}$ .

The average low-pressure local cluster sizes, shown in Fig. 3, are consistent with topologies intermediate between those of cristobalite-like (69 atoms in a putative Ge-centered cluster) and quartz-like (155 atoms in a Ge-centered cluster) structures, whereas the local cluster size of the high-pressure structure is closer to that of rutile-like topologies (53 atoms in a Ge-centered cluster). The local increase again at around  $4500 \text{ kg/m}^3$  is consistent with the rapid rise of quartz-like 8-rings at this density and reversion to a quartz-like accommodation of increased density. The highest-pressure ring-size distribution is particularly notable in that a substantial population of 2-, 3- and 4-rings appears, consistent with the ring-size distribution of rutile.

The conclusion is that imposition of pressure effects two *separate* accommodating responses in the structure of germania glasses: at first, the intermediate-range tetrahedral network structure responds by transforming to one with larger rings (and larger ring clusters) that can more readily accommodate the imposed density increase; then, with those options exhausted, the local short-range co-ordination changes from tetrahedral (four oxygens around Ge)



to octahedral (six oxygens around Ge, as shown in Fig. 1), with an intermediate fivefold co-ordinated state. The result is an even denser packing of atoms in the structure, with associated implications for intermediate-range structure, such as edge-sharing connectivities.

The final structure at the highest density simulated,  $6000 \text{ kg/m}^3$ , cannot be uniformly rutile-like, because of the continued dominance of 6-rings, despite the near-6:3 co-ordination. This result is not entirely surprising, since the extrapolated density of the rutile-structure analogue of crystalline  $\text{GeO}_2$  is  $6251 \text{ kg/m}^3$  [26] in excess of the final model density of  $6000 \text{ kg/m}^3$ , and the final average Ge co-ordination is 5.7, not 6. That said, the present modelling parameters may also have affected the result. Simulated glasses unavoidably have much higher glass transition temperatures due to the extremely fast quench rates in MD simulation. This implies that simulated glass structures are much less equilibrated than experimental ones and hence may contain significant fractions of remnant structures that were unable to adjust themselves in a timely manner (a memory effect). It is possible that a well equilibrated (many more iteration steps) larger simulation system (several thousand atoms) would deliver more rutile-like structures. Additionally, the rather small simulation size (864 atoms) of the present study may have had incorporated non-negligible translational boundary-condition restraints. Such restraints add additional barriers for atoms to adjust appropriately and thus could have hindered the transition to a more rutile-like structure.

## 5. Conclusion

We have presented in this contribution a study of short- and intermediate-range structures in densified  $\text{GeO}_2$  glass, modelled using molecular dynamics with an empirical potential and analyzed using a topological approach. The results suggest that germania glasses may accommodate imposed density change under pressure by adjustments in both short-range and intermediate-range structure that are not necessarily connected. The latter appear to be more readily adopted and yield to short-range co-ordination changes only when their capacity to effect significant further density change is exhausted. The rich information obtainable from this single set of simulations portends substantial new understanding about glass structure options that should be confirmed by a forthcoming systematic set of much larger simulations that will reduce the parameter scatter. Correlation to possible experimental signatures of topological structure (such as the first sharp diffraction peak in X-ray and neutron scattering [32]) is being investigated.

## Acknowledgements

It is a pleasure for MM to acknowledge discussions with G. Calas, L. Cormier, G. Ferlat, B. Guillot, Y. Guissani,

G. Hovis and P. Richet. XY and LWH gratefully acknowledge the support of the Cambridge-MIT Institute.

## References

- [1] M. Guthrie, C.A. Tulk, C.J. Benmore, J. Xu, J.L. Yarger, D.D. Flug, J.S. Tse, H.K. Mao, R.J. Hemley, *Phys. Rev. Lett.* 93 (2004) 115502.
- [2] S. Sampath, C.J. Benmore, K.M. Lantz, J. Neuefeind, K. Leinenweber, D.L. Price, J.L. Yarger, *Phys. Rev. Lett.* 90 (2003) 115502.
- [3] P.S. Salmon, R.A. Martin, Ph. Mason, G.J. Cuello, *Phys. Rev. Lett.* 96 (2006) 235502.
- [4] C.E. Stone, A.C. Hannon, T. Ishihara, N. Kitamura, Y. Shirakawa, R.N. Sinclair, N. Umesaki, A.C. Wright, *J. Non-Cryst. Solids* 293–295 (2001) 769.
- [5] L.W. Hobbs, C. Esther Jesurum, Bonnie Berger, The topology of silica networks, [Chapter 1], in: J.-P. Duraud, R.A.B. Devine, E. Dooryhee (Eds.), *Structure and Imperfections in Amorphous and Crystalline Silica*, John Wiley, London, 2000, p. 1.
- [6] A. Polian, M. Grimsditch, *Phys. Rev. B* 41 (1990) 6086.
- [7] S. Sugai, H. Sotokawa, D. Kyolane, A. Onodera, *Physica B* 219 (1996) 293.
- [8] C.H. Polsky, K.H. Smith, G.H. Wolf, *J. Non-Cryst. Solids* 248 (1999) 159.
- [9] K.H. Smith, E. Shero, A. Chizmeshya, G.H. Wolf, *J. Chem. Phys.* 102 (1995) 6851.
- [10] G.S. Henderson, H. Wang, *Eur. J. Mineral.* 14 (2002) 733.
- [11] J.P. Itié, A. Polian, G. Calas, J. Petiau, A. Fontaine, H. Tolentino, *Phys. Rev. Lett.* 63 (1989) 398.
- [12] S. Sugai, A. Onodera, *Phys. Rev. Lett.* 77 (1996) 4210.
- [13] R.J. Hemley, C. Meade, H.K. Mao, *Phys. Rev. Lett.* 79 (1997) 1420.
- [14] M. Micoulaut, L. Cormier, G.S. Henderson, *J. Phys. Condens. Mater.* 18 (2006) R753.
- [15] R.D. Oeffner, S.R. Elliott, *Phys. Rev. B* 58 (1998) 14791.
- [16] M. Micoulaut, *J. Phys. Condens. Mater.* 16 (2004) L131.
- [17] M. Micoulaut, Y. Guissani, B. Guillot, *Phys. Rev. E* 73 (2006) 031504.
- [18] K. Kamiya, T. Yoko, Y. Itoh, S. Sakka, *J. Non-Cryst. Solids* 86 (1985) 385.
- [19] X. Yuan, A.N. Cormack, *Comp. Mater. Sci.* 24 (2002) 343.
- [20] L.W. Hobbs, C.E. Jesurum, V. Pulim, B. Berger, *Philos. Mag.* A 78 (1998) 679.
- [21] X. Yuan, L.W. Hobbs, NetAnal: A freeware structural network analysis tool, in: 13th International Conference on Radiation Effects in Insulators, Santa Fe, NM, 28 August–2 September 2005.
- [22] C.S. Marians, L.W. Hobbs, *J. Non-Cryst. Solids* 119 (1990) 269;
- [23] C.S. Marians, L.W. Hobbs, *J. Non-Cryst. Solids* 124 (1990) 242.
- [24] K.V. Shanavas, G. Nandini, S. Sharma, *Phys. Rev. B* 73 (2006) 094120.
- [25] L. Giacomazzi, P. Umari, A. Pasquarello, *Phys. Rev. B* 74 (2006) 155208.
- [26] L.W. Hobbs, Xianglong Yuan, Topology and topological disorder in silica, in: G. Pacchioni, L. Skuja, D.L. Griscom (Eds.), *Defects in  $\text{SiO}_2$  and Related Dielectrics: Science and Technology*, Kluwer, Dordrecht, Netherlands, 2000, p. 37.
- [27] T. Yamanaka, K. Ogata, *J. Appl. Crystallogr.* 24 (1991) 111.
- [28] G.S. Henderson, M. Fleet, *J. Non-Cryst. Solids* 134 (1991) 259.
- [29] F.L. Galeener, A.J. Leadbetter, M.W. Stringfellow, *Phys. Rev. B* 27 (1983) 1052.
- [30] A. Pasquarello, R. Car, *Phys. Rev. Lett.* 80 (1998) 5145.
- [31] D.J. Durben, G.H. Wolf, *Phys. Rev. B* 43 (1991) 2355.
- [32] L. Giacomazzi, P. Umari, A. Pasquarello, *Phys. Rev. Lett.* 95 (2005) 075505.
- [33] L.C. Qin, L.W. Hobbs, *J. Non-Cryst. Solids* 192&193 (1995) 456.